

Resuspension of sediment in a semi-sheltered bay due to wind waves and fast ferry wakes

Ants Erm*, Victor Alari, Inga Lips and Jüri Kask

*Marine Systems Institute at Tallinn University of Technology, Akadeemia tee 21, EE-12618 Tallinn, Estonia (*corresponding author's e-mail: ants@phys.sea.ee)*

Received 4 Dec. 2009, accepted 18 Sep. 2010 (Editor in charge of this article: Kai Myrberg)

Erm, A., Alari, V., Lips, I. & Kask, J. 2011: Resuspension of sediment in a semi-sheltered bay due to wind waves and fast ferry wakes. *Boreal Env. Res.* 16 (suppl. A): 149–163.

Concurrently with the wind wave induced sediment recycling, large sections of the coast of Tallinn Bay are influenced by wakes generated by high speed vessels. Based on *in situ* measurements of surface waves, underwater irradiance and the fluxes of resuspended sediment, combined with counting of particles with FlowCAM and numerical modeling of wind waves, it is shown, that the anthropogenic resuspension plays a key role in the western part of Tallinn Bay during the relatively calm spring and summer seasons. The near bottom orbital velocities generated daily by fast ferries' wakes are equivalent to those induced by wind waves excited by at least 18 m s^{-1} southwestern winds and 12 m s^{-1} northern winds. About 400 kg of sediment is resuspended and carried away from each meter of coastline annually.

Introduction

The concentration and distribution of suspended matter is important in several aspects. Together with dissolved organic (yellow) matter and phytoplankton, the (re)suspended matter affects the quality of a body of water (Lawrence and Herbert 1968, Floderus *et al.* 1999, Booth *et al.* 2000, Effler *et al.* 2002, Wild-Allen *et al.* 2002, Binding *et al.* 2003, 2005, Dierssen *et al.* 2009). Sediment resuspension events alter the concentration of dissolved phosphorus, with suspended solids acting either as its sink or source. Light attenuation also changes with the variations of the concentration of suspended solids. These effects may be reflected in the abundance and species composition of phytoplankton and macrophyte communities in coastal environments. Alterations in the sediment resuspension regime

may also cause changes in the bottom topography. The effect of wind waves on the suspended solids concentration in coastal environments is well documented (Booth *et al.* 2000, Jönsson 2006).

Tallinn Bay is a small coastal environment located in the southern Gulf of Finland (Baltic Sea) (Fig. 1). Due to the islands surrounding the bay and the shallows located at its entrances, the intensity of the wind wave field in the bay interior is quite limited (Soomere 2005a). As a result, wind-wave-induced sediment resuspension events apparently are also very limited. However, the bay has another driving force for sediment resuspension.

For the last ten years, high-speed crafts (HSC) and high-powered large vessels (hereafter called fast ferries) have been extensively used in the passenger traffic between Tallinn and Hel-

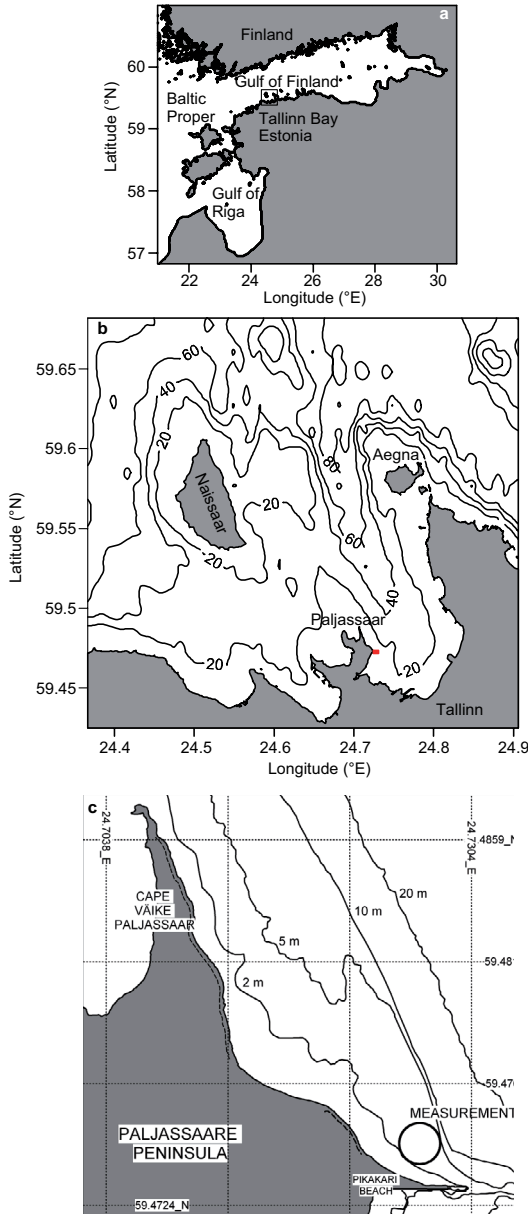


Fig. 1. (a) Study area, (b) the topographic map of Tallinn Bay, and (c) bathymetry and location of the measurement area.

sinki. Nowadays, only fast ferries have remained in the fleet of vessels sailing with speeds considerably greater than characteristic to conventional ferries (20–21 knots). In summer 2009, three fast ferries were operating in Tallinn Bay: *Tallink Star* and *Tallink SuperStar* (Tallink) and *Viking XPRS* (Viking Line). These almost 200-m-long

ferries with an engine power of 40 000–50 000 kW have 2000 lane meters for vehicles, accommodate 1900–2500 passengers and can develop a speed of up to 27 knots (Parnell *et al.* 2008).

Already in the early 2000s, various adverse impacts of the wakes generated by HSCs and fast ferries were reported in this area (Peltoniemi *et al.* 2002, Soomere and Kask 2003, Soomere *et al.* 2003, Erm and Soomere 2004). A significant number of measurements of waves had been conducted near the eastern coast of Tallinn Bay, mainly near Aegna Island (Soomere and Rannat 2003, Soomere *et al.* 2005, Soomere 2005b, 2006, Torsvik and Soomere 2008, Parnell *et al.* 2008, Torsvik *et al.* 2009, Didenkulova *et al.* 2009, Kurennoy *et al.* 2009a, 2009b, Alari *et al.* 2009a, Kelpšaitė and Soomere 2009). The results showed, that the wakes generated by fast ferries and HSC in Tallinn Bay had several properties (the waves were substantially non-linear, high, long, long-crested and exerted very high run-up), usually not typical for wind-generated waves. Measurements of the impact of ship wakes on the optical properties of seawater together with studies of sediment transport began in 2003 (Erm and Soomere 2004) and are still ongoing (Erm and Soomere 2006a, 2006b, Erm *et al.* 2006, 2008, 2009). These investigations showed that ferries and HSC wakes were able to resuspend huge amounts of sediments and considerably affect the underwater light climate.

Numerical simulations (Torsvik and Soomere 2008, Torsvik *et al.* 2009) suggest that the wakes from fast ferries sailing to Tallinn may strongly impact the western coast of Tallinn Bay, in particular the eastern coast of Kopli Peninsula. Observations from the coast and reports from seamen indicate that ship wakes may cause extensive damage in this area (Jõevere 2003).

In this paper, we present results of recent studies of the properties of wakes from fast ferries and their impact performed in the neighborhood of Pikakari Beach and Katariina Jetty located on the western coast of Tallinn Bay. Our basic goal is to estimate the potential effect of the fast ferry wakes for sediment resuspension processes in this area based on synchronous measurements of wave properties, underwater irradiation and vertical and horizontal fluxes of sediment.

Methods

Geological setting of the study site

The study area is located in the eastern part of Paljassaare Peninsula, north of Katariina Jetty (Fig. 1). The complex geometry of the shoreline of the inner part of Tallinn Bay together with a variable composition of its geological setting create preconditions for large spatial variations in the distribution of sedimentary material depending on the position of peninsulas and bays. The Lower-Cambrian bedrock is mainly overlain here by glacial till and post-glaciation's marine sediments. The till is rich in sediment particles originating from the bedrock. This accounts for the high content of clay and silt in the shore and shoreface sediments. Abundant crystalline pebbles and cobbles often occur in the till (Kink and Raukas 1998, Saarse and Vassiljev 2008). As some 3000 years ago the area of present-day Paljassaar Peninsula was seafloor (Saarse and Vassiljev 2008), the till is overlain by relatively young, unconsolidated marine sediment (sand, gravel and pebbles).

The shore section southward of Katariina Jetty has been under severe human impact. The jetty is a ca. 300-m-long east-westerly-oriented structure, with concrete blocks piled at its northern side and around the seaward tip to protect the jetty. Near its seaward tip the water depth reaches 2 m. A triangular sandy deposition feature at the northern side of the jetty is known as Pikakari Beach (Fig. 2). The sandy area is approximately 200 m long and ends abruptly as the character of the beach changes (Fig. 2). In the landward part of this beach partially vegetated foredunes occur, providing evidence of intensive accumulation and aeolian processes.

Near the study area, in the nearshore and at depths 5–10 m there is a quite steep scarp accreted in bedrock, formed of blue clay, siltstone and sandstone. Also pebbles (mostly crystalline) occur sporadically. Among those, there are also rounded red brick pebbles originating from the facilities established on Cape Väike-Paljassaar during World War I. Their remains can be found ca. 1.5 km northwestward on the backshore.

To the north from Pikakari Beach, the shoreline runs in the northwestern direction. North-



Fig. 2. View towards Katariina Jetty in 2009. The border between till shore and sandy beach is relatively sharp (photo by A. Kask).

west of the beach the backshore is bordered with a scarp eroded in till. The shore is covered with residual sediments left by the retreating till scarp and is dominated by coarser sediments — medium and coarse sand, pebbles, cobbles and boulders. The majority of fine-grained sediments such as clay, silt and fine sand have been transported either southwards or deeper into the sea.

Wave measurements

A wave gauge, which measures the dynamic pressure with a sampling frequency of 4 Hz, was deployed at a water depth of 3.6 m near Katariina Jetty on the late evening of 20 July and was retrieved at 10:00 on 23 July. In order to resolve the information about high frequency wind waves, the gauges were placed at a height of 2.1 m from the sea bed. Air pressure was first subtracted from the raw pressure time-series. The low-frequency oscillations of the sea level were filtered out by dividing the time-series into 5-minute-long sections, which were de-meaned and de-trended separately. The resulting attenuated pressure fluctuations at a given depth were converted to water level fluctuations (that is, to surface gravity waves) using the linear wave theory.

For each 5-minute-long section of time-series of surface elevation, the maximum wave height and the associated wave period was determined using the zero-downcrossing method. From the wave period and water depth, the wavelength

was derived according to the linear dispersion equation. The near bottom orbital speed was calculated as the ratio of the near-bottom excursion amplitude and wave period according to the classical linear wave theory. Due to high crest-trough asymmetry of the leading waves from fast ferries (Soomere *et al.* 2005, Kurennoy *et al.* 2009a, 2009b), the maximum near bottom orbital velocities due to the largest fast ferry wakes presented in this paper apparently are considerably underestimated (Soomere *et al.* 2005, Alari *et al.* 2009a) and should be treated as minimum values induced by fast ferry wakes.

No measurements of wind waves have been conducted near Katariina Jetty or near the western coast of Tallinn Bay. Although Soomere (2005a) established the statistical properties of Tallinn Bay's natural wave fields with the use of the WAM model, no information is available for the area in question about the associated the near-bottom velocities for particular wind conditions. Alari *et al.* (2009b) verified the SWAN model (Booij *et al.* 1999) with the new saturation scheme (that more adequately accounts for dissipation owing to whitecapping, Van der Westhysen *et al.* 2007) against thousands of hours of measurements. They found that in suitable forcing conditions, the model reproduces the wave properties well even in very complex places like shallow coastal waters or banks. This model was used to assess the potential sediment resuspension characteristics near Katariina Jetty due to wind waves corresponding to a discrete set of wind speeds of 6 m s⁻¹, 12 m s⁻¹ and 18 m s⁻¹ and for 16 directions with a spatial resolution of 463 m. The details of model topography and basic equations can be found in Alari and Raudsepp (2010).

In practice, none of the model grid points exactly coincides with the locations of the measurement site. The nearest SWAN grid point is located about 300 m east of the measurement point. The water depth at this grid point is 12 m whereas at the measurement point it was 3.6 m. As the waves propagate towards the coast, the wave periods do not change but heights tend to increase due to the shoaling effect. At the same time, wave energy is being damped by the dissipation due to bottom friction in the coastal zone. These two mechanisms frequently balance each other. To a first approximation, it may, therefore,

be assumed that the wave which propagates from the model grid point to the measurement point keeps its period and height. The wavelength for estimates of the orbital speed is calculated for the water depth of 3.6 m at the measurement site.

Underwater irradiation

To measure the underwater light field, we used a set consisting of two underwater radiometers Ramses-ACC-VIS (Trios GmbH, Germany) positioned on the same frame at the elevations of 0.5 m and 1 m from the sea bed. It allowed for measuring the spectral profiles of underwater irradiation $E_d(\lambda)$ as well as the vertical profiles and temporal variation of diffuse attenuation coefficient in the range from 320 nm to 950 nm. The diffuse attenuation coefficient (Dera 1992)

$$K_d(z) = \frac{d}{dz} \ln E_d(z) = \frac{1}{E_d(z)} \frac{dE_d(z)}{dz} \quad (1)$$

characterizes the attenuation rate of the downwelling irradiance at a certain depth z . The larger is this coefficient, the less light penetrates to the deeper layers. An approximate average value of K_d in the water layer between the sensors can be calculated as

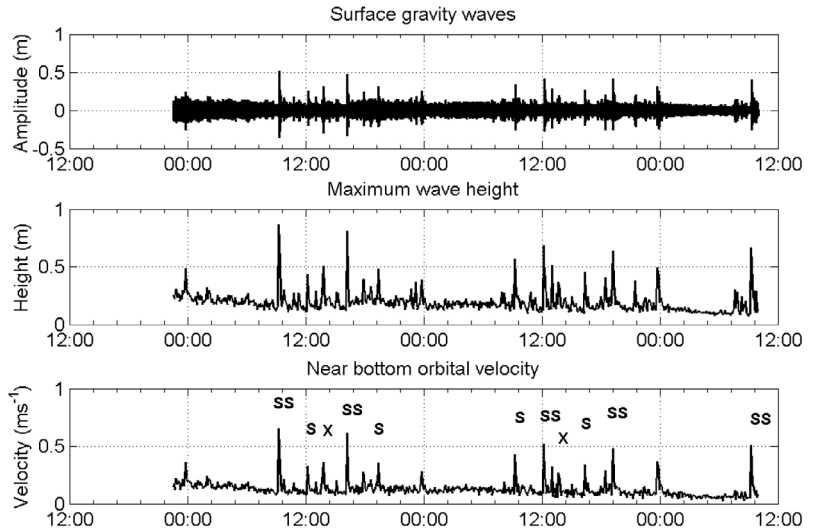
$$K_d\left(\frac{z_1 + z_u}{2}\right) = \frac{1}{z_1 - z_u} \ln \frac{E_d(z_1)}{E_d(z_u)} \quad (2)$$

where $E_d(z)$ is measured at the depths z_u (upper sensor) and z_1 (lower sensor). The theoretical basis of determination of the properties of resuspension by means of such optical measurements is described in detail by Erm *et al.* (2009).

Sediment traps

The intensity of sediment resuspension was quantified using two types of experimental sediment traps. The first one was used to determine downwelling sediment fluxes at different elevations. This set consisted of four funnels (\varnothing 13.5 cm) mounted onto a diving frame. Particles falling down were caught into 0.5 l removable sampling bottles. The catching levels were adjusted to elevations 0.5 m, 0.8 m, 0.9 m and 1.1 m from the sea bed.

Fig. 3. Surface wave parameters on 21, 22 and 23 July 2009 measured near Katariina Jetty. Upper panel represents the fluctuation of waves plotted for every 0.25 s; for the middle and lower panel the values are maxima occurring in 5 minute time interval. SS = Tallink SuperStar, S = Tallink Star and X = Viking XPRS.



The second set ($9.5 \times 9.5 \text{ cm}^2$ each trap) was used to measure the horizontal flux of sediment at two different heights (0.2 m and 0.5 m above the sea bed) and in two directions (seaward and shoreward). Plankton nets were used to catch the sediment. The fluxes of sediment were calculated based on the dry weight of captured sediments, sampling duration and cross-sections of the traps.

Imaging and counting of particles

The sediments caught on 21–23 July during a 50.5 h time interval were analysed using an imaging flowcytometer FlowCam (Fluid Imaging Technologies, Edgecomb, Maine, USA), which measures particles from 2–2000 μm . From each sediment sample (taken from four elevations), particles in a 5 ml probe were counted and imaged. The relevant method is described in (Sieracki *et al.* 1998). Designed primarily for phytoplankton analysis, this instrument is seldom used for sediment aggregate analysis. However, as the image analysis program provides projected area and maximum length data for each measured particle, data from FlowCAM can be used to determine the distribution of fractions of particles of different shape and size (Sterling *et al.* 2004).

In experiments, only a part of the potential measurement range of the system was used. The

probes were analysed by using a 2 mm wide and 0.1 mm thick flow cell and a 20 \times magnification objective ($0.67 \mu\text{m}$ per pixel). The samples were pre-filtered through a 300 μm sieve to avoid clogging of a flow cell. As no significant amount of bigger particles remained on a sieve, this limitation insignificantly affects the results of the analysis. The equivalent volume (called bio-volume in phytoplankton research) of each particle was calculated from its equivalent spherical diameter (ESD).

Results and discussion

Waves

A diurnal cycle of waves with a low background value at nights and higher wave events during daytime was observed in measurements (Fig. 3). According to the HIRLAM model results, on the nights of 21 and 22 July the wind in Tallinn Bay was blowing from SSW–SW with a speed of about 7–9 m s^{-1} . This resulted in the maximum values of the wind wave height (0.20–0.25 m on average) near Katariina Jetty during the measurement period. As the wind speed decreased below 5 m s^{-1} on the night of 23 July, the maximum wave height was less than 0.15 m. The corresponding values of near bottom orbital velocities were on average 0.15 m s^{-1} on the night of 21 July and below 0.1 m s^{-1} during the following nights.

Although the events of the fast ferry wakes varied in height during the measurement, their period remained between 7–8 s. The daily largest ship waves were clearly higher than 0.65 m. The highest ship wave (0.85 m) was measured at about 09:20 on the morning of 21 July. A somewhat smaller wave, with a height of 0.8 m, was recorded in the afternoon of the same day. The highest wakes were generated by *Star* or *SuperStar*, rather than *XPRS*. The near bottom velocities generated by fast ferries were clearly over 0.3 m s^{-1} whereas their daily maxima reached 0.5 m s^{-1} . Evidently, the maximum flow velocities over 0.6 m s^{-1} correspond to waves with maximum heights on 21 July.

The periods of the leading waves generated by fast ferries coincide with the ones established from similar measurements near Aegna Island (Erm *et al.* 2008, 2009, Parnell *et al.* 2008), but the maximum heights are by 0.3 m lower on average. This clearly demonstrates that although the ship wave height may vary in different locations and may depend on the sailing direction and thus wave generation conditions, the wave period of wakes from *Star*, *Superstar* and *Viking XPRS* insignificantly changes. The latter feature is consistent with the general opinion that the wave period depends mainly on the ship's speed and the water depth at the generation area (Torsvik and Soomere 2008).

According to model calculations, SW winds with a speed 9 m s^{-1} excite the significant wave height about 0.3 m in the neighbourhood of the measurement site, which matches well the measured values. North wind with a speed of 6 m s^{-1} creates wave fields with the significant wave height below 0.35 m and the peak period less than 3 s. When the wind speed increases to 12 m s^{-1} , the modelled significant wave height increases to 1 m and the peak period is about 5 s. North winds with a speed of 18 m s^{-1} generate 1.7 m high waves with peak periods of up to 7 s. However, for the west winds with a speed of 12 m s^{-1} , the significant wave height is 0.5 m and the peak period is 6.5 s. As the measurement site is sheltered from this direction, the predominant waves approaching the study area must have undergone significant refraction.

Winds with 6 m s^{-1} from SW generate near bottom orbital velocities below 0.01 m s^{-1} . For

wind speeds 12 m s^{-1} and 18 m s^{-1} these values are 0.2 m s^{-1} and 0.5 m s^{-1} , respectively. North winds with speeds 6, 12 and 18 m s^{-1} generate near bottom velocities 0.1, 0.6 and 1.1 m s^{-1} , respectively. Thus, the maximum near bottom orbital velocities generated by fast ferries are equivalent to those induced by north winds exceeding 12 m s^{-1} or SW winds exceeding 18 m s^{-1} . In Tallinn Bay, 6 m s^{-1} is a typical wind speed in autumn and winter (Prilipko 1982). As the mean wind speed during spring and summer months is 3–4 m s^{-1} , the background of wind waves is almost negligible during these seasons. According to the HIRLAM model output, in 2006–2009 the frequency of winds $\geq 12 \text{ m s}^{-1}$ did not exceed 6.4% and the share of winds $\geq 18 \text{ m s}^{-1}$ was 0.1% (Alari *et al.* 2009a). Based on the above, it may be concluded that resuspension of sediment at the measurement site is due to fast ferry wakes rather than wind waves. This feature obviously reflects the sheltered nature of Tallinn Bay, because in the Baltic Proper waves caused by winds with a speed of 5 m s^{-1} can already resuspend sediments (Jönsson 2006).

Optical method for estimation of a wake impact

The underwater light irradiance $E_d(\lambda)$ was monitored in the morning of 21 July. A vertical profile $E_d(\lambda, z)$ was measured before the first ferry from Helsinki passed the measurement site. To a first approximation, the mean background values of diffuse attenuation coefficient $K_d(\lambda)$ for the whole water column are calculated from the profiles $E_{d,\lambda}(z)$ originating from Eq. 1 ($E_{d,\lambda}(z) = E_{d,\lambda}(0)e^{-K_{d,\lambda}z}$, where $E_{d,\lambda}(0)$ is a constant equivalent to the irradiation just under the water) presented in Fig. 4.

The impact of a fast ferry wake on the irradiation properties at two levels — 0.5 and 1.0 m from the sea bed — was established from measurements performed from 09:01 to 09:41 at the 1/60 Hz sampling rate. During this time interval, a strong wake from *SuperStar* sailing to Tallinn (scheduled arrival 09:30) reached the study site. The values of $K_d(\lambda)$, calculated from $E_d(\lambda)$ spectra (Fig. 5) showed that the transparency of water was highest at wavelengths 500–600 nm

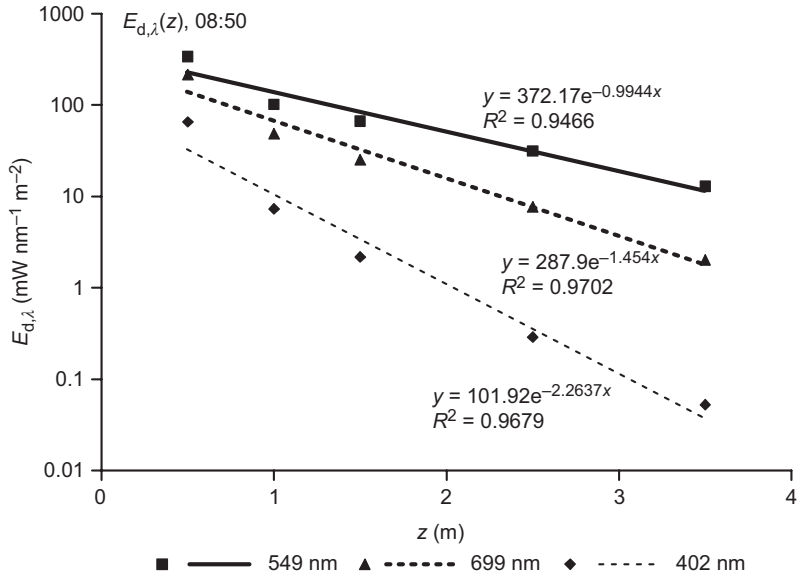


Fig. 4. Depth dependence of $E_{d,\lambda}$ at three wavelengths in the morning of 21 July 2009 before the arrival of ferries from Helsinki.

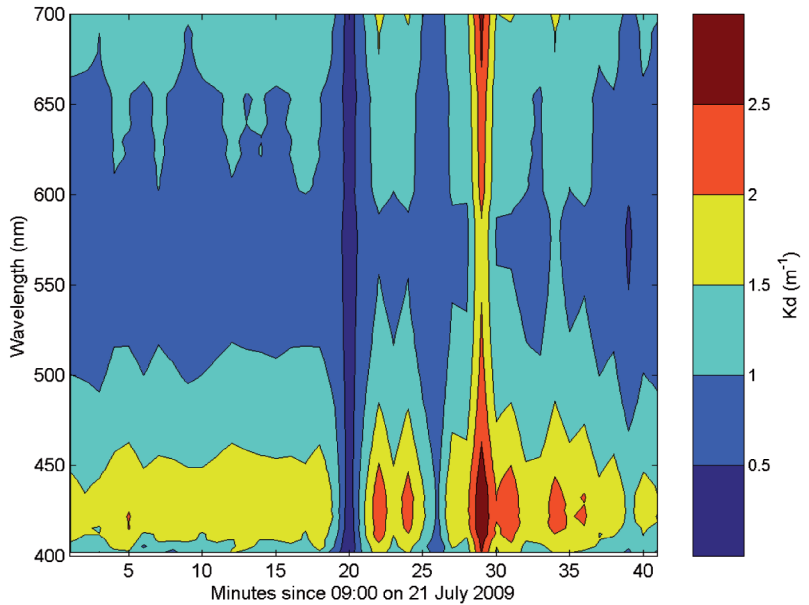


Fig. 5. Diagram of diffuse attenuation coefficient $K(\lambda, t)$ of the water layer 0.5–1.0 m from the sea bed in the morning of 2 July 2009.

whereas the impact of the wake was evident in the entire range of light wavelengths.

Generally, light attenuation in the sea water depends on the pure sea water characteristics and concentrations of optically active substances (Devlin *et al.* 2008):

$$K_d(\lambda) = a_w(\lambda) + b_w(\lambda) + K'_{d,y}(\lambda)C_y + K'_{d,chl}(\lambda)C_{chl} + K'_{d,s}(\lambda)C_s, \quad (3)$$

where $a_w(\lambda)$ and $b_w(\lambda)$ are the absorption and backscattering of pure sea water (Smith and Baker 1981), C_y , C_{chl} and C_s are the concentrations of yellow substance, chlorophyll and suspended matter, respectively; $K'_{d,y}(\lambda)$, $K'_{d,chl}(\lambda)$ and $K'_{d,s}(\lambda)$ are the empirical attenuation cross-sections of yellow substance, chlorophyll and suspended matter.

In order to quantify the magnitude of resus-

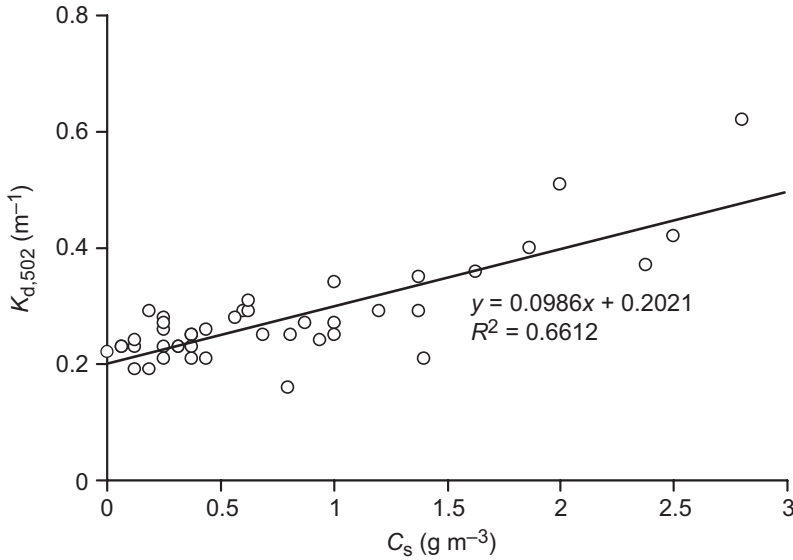


Fig. 6. Dependence of diffuse attenuation coefficient at 502 nm ($K_{d,502}$) on concentration of suspended matter (C_s) in Tallinn Bay in years 2009–2010. The slope of the plot corresponds to the value of $K'_{d,s,502}$.

pension events based on optical measurements it is necessary to understand how $K_d(\lambda)$ depends on C_s . It can be assumed that the concentration of yellow substance is not influenced by waves and wakes. Phytoplankton has nearly the same density as the sea water and is, especially under dynamic conditions such as wind waves and ferries' wakes mostly floating in the water column. Therefore, C_{chl} also could be taken as a constant value during the measurement period (only a part of an astronomical day in most cases). On the other hand, yellow substance is absorbing light in the ultraviolet (UV) and blue ranges of the spectrum, and the mean absorption maximum of chlorophyll is at 665 nm. Therefore, at wavelengths between 500–600 nm both yellow substance and chlorophyll have a marginal effect on the attenuation spectra. Consequently, Eq. 3 can be rewritten as:

$$C_s = \frac{1}{K'_{d,s,\lambda}} (K_{d,\lambda} - K), \quad (4)$$

where $K'_{d,s,\lambda}$ is the cross-section of suspended matter at a wavelength λ (between 500–600 nm), and K is a constant describing all attenuation components except the one for suspended matter.

Similarly with the measurements in the photosynthetically active range (PAR) (Erm and Soomere 2006) the impact of a ferry wake can be quantitatively described as

$$M_f = \frac{1}{K'_{d,s,\lambda}} \int_{t_1}^{t_2} |K_{d,\lambda}(t) - K_{d0,\lambda}(t)| dt, \quad (5)$$

where M_f (g s m^{-3}) characterizes the impact of wakes over some period $\Delta t = t_2 - t_1$, and $K_{d0,\lambda}(t)$ is a background value of the diffuse attenuation coefficient.

According to Eq. 4, $K'_{d,s,\lambda}$ can be estimated from the values of $K_{d,\lambda}(C_s)$ similarly as it was done for $K'_{d,s,PAR}$ by Erm and Soomere (2004). In 2009 and 2010, five measurement sessions were performed in sand dredging areas in Tallinn Bay. Spectral profiles of underwater light were measured using the above-described Ramses radiometer and the concentration of suspended matter was determined from water samples. The dependence of attenuation of light at 502 nm $K_{d,502}$ on C_s is presented in Fig. 6. The slope of linear regression for the values of $K_{d,502}(C_s)$ was used as $K'_{d,s,\lambda}$ for 502 nm ($\sim 0.1 \text{ m}^2 \text{ g}^{-1}$) in Eq. 5.

To estimate the total impact of a wake, $K_{d,502}(t)$ was compared with the surface wave time-series for the same time period (Fig. 7). This quantity showed almost no variations during the first 18 minutes of the record before the arrival of the ferry wake (Fig. 6a). Its mean value during the first 18 minutes (1.1 m^{-1}) is used as a reference value $K_{d0,\lambda}(t)$ in Eq. 5 for calculating the impact of the wake. The overall minimum of $K_{d,502}$ (0.28 m^{-1}) occurred at 09:20. After some increase its

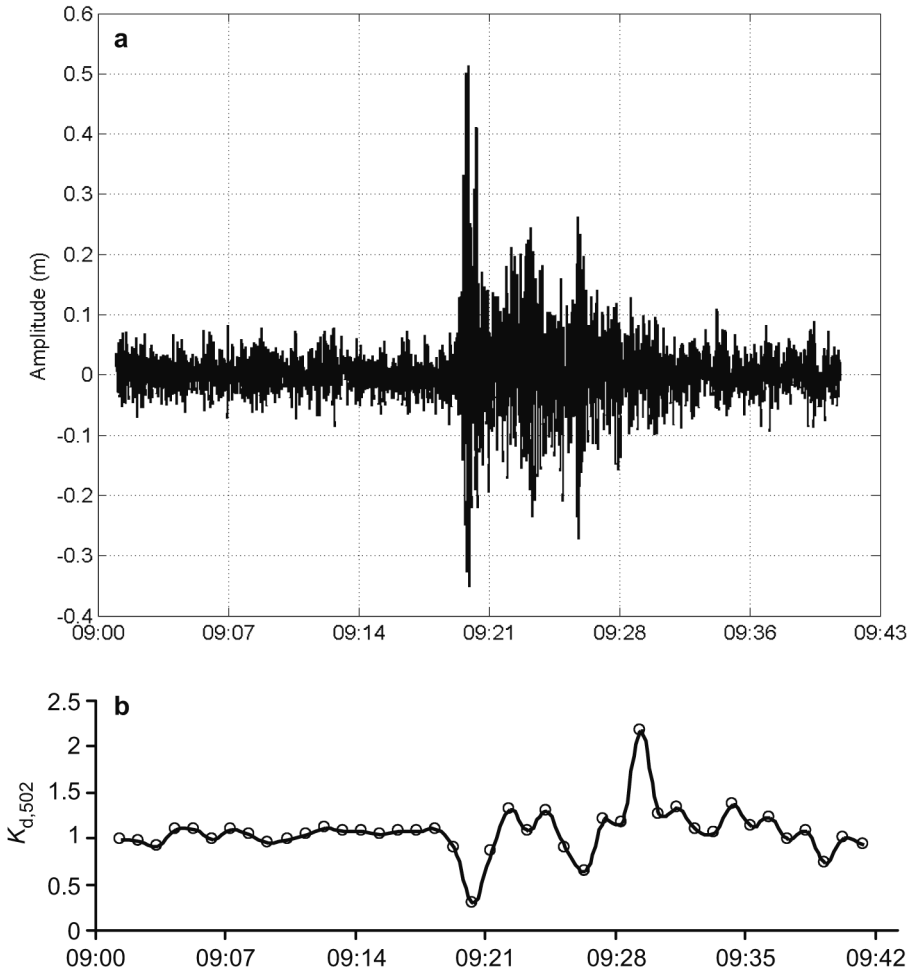


Fig. 7. (a) Wave amplitude and (b) $K_{d,502}(t)$ caused by *Tallink SuperStar* in the morning of 21 July 2009.

values dropped again, to a value of 0.63 m^{-1} . This minimum of $K_{d,502}(t)$ occurs when the leading wave of *SuperStar* reached the study site (Fig. 7b). Such a decrease may reflect so-called ventilation of near-bottom water layer (that the wakes bring clear water into the lower water layers) that was also observed near Aegna Island in Tallinn Bay by Erm *et al.* (2006). Further on, $K_{d,502}(t)$ substantially increased to 2.17 m^{-1} and then decreased in a slightly oscillating manner back to the mean value.

The larger sediment fractions stay mostly in the lower layer, while the finer components sediments may be resuspended to higher layers. The local maximum at 09:22 when $K_{d,502}$ increased to 1.32 m^{-1} probably reflects the settlement of heavier fraction of sediments, while the maximum at

9:29 is the result of lighter fraction settlement.

The 'total impact' of this wake established by means of Eq. 5 is $M_{SS} = 2654 \text{ g s m}^{-3}$. It is 1.6–1.8 times as high as than the mean values calculated for *Tallink AutoExpress* and *Super-SeaCat* (1649 g s m^{-3} and 1483 g s m^{-3} , respectively) for years 2003–2004 near Aegna Island (Erm and Soomere 2006). Assuming the impact time of all three ferries being the same (~22 min) and taking into account that *SuperStar* and *Star* were passing the measuring station (on average) 2.5 times and *XPRS* twice daily, the 'total impact' of all ferries was $10\,350 \text{ g s m}^{-3}$. Total impact $13\,000$ – $14\,000 \text{ g s m}^{-3}$ for a 5.5 h period was calculated for the nearshore of Aegna in the years 2003–2005 (Erm and Soomere 2006b, Erm *et al.* 2006). Mean excess concentrations

of resuspended sediments induced by a ferry calculated as $\Delta C_s = M_f / \Sigma \Delta t$, where $\Sigma \Delta t$ is the sum of impact periods in a day, were 2.0, 0.8 and 0.4 g m⁻³ (for *SuperStar*, *Star* and *XPRS*, respectively). For the period of 2003–2004 its mean values of 2.3 (*AutoExpress*) and 3.3 g m⁻³ (*SuperSeaCat*) were calculated for much smaller but faster ferries near Aegna Island (Erm and Soomere 2006a).

Another comparison could be made based on assumptions that the excess transport of sediment occurs in about 1 m deep near-bottom water layer ($h \approx 1$) (Erm et al. 2006) and that the characteristic coastal current speed v in Tallinn Bay is about 0.1 m s⁻¹ (Orlenko 1984, Erm et al. 2008). The total mass of sediment m_v brought into motion per each meter of the affected coastline sections within a navigation day can be estimated as

$$m_v = vh \Sigma M_f = 10\,350 \text{ (g m}^{-1}\text{)}, \quad (6)$$

what is 3.6 times lower as estimated for the near-shore of Aegna for 2005. If 10% of this amount will be carried out of the bay or accumulated in deeper sea areas, during one navigation period the net loss of fine sediments could be about 400 kg m⁻¹.

Of course, all these comparisons should be treated as indicative. First of all, they are based on very rough approximations and on a limited data set. As the bathymetry and sediment properties are different in these two measurement states, the resuspension and transport properties are obviously different.

Sediment fluxes

Resuspended particles were periodically captured with sediment traps during 18 June–28 July 2009. The rate of resuspension was calculated with the following formula:

$$F_{\text{tot}} = \frac{m}{S t_{\text{tot}}}, \quad (7)$$

where F_{tot} is the total flux of sediments (incorporating both the flux induced by wind waves and the flux generated by ferry wakes), m (g) is the dry weight of captured sediments, S (m²) is the cross-section of the trap, and t_{tot} (h) is the duration of sampling.

Experiments were carried out using horizontal sediment traps placed at two different elevations (0.2 and 0.5 m from the sea bed) and arranged in two different directions (seaward and shoreward). The results showed that a 0.3 m increase in elevation plays a critical role in the rate of sediment supply to the water column — the fluxes at 0.2 m were up to an order of magnitude higher than those at 0.5 m (Table 1). On the average, the seaward flux was 1.3 times as large as the shoreward one.

Two sources contribute to the locally resuspended sediment flux — wind waves and ship wakes. To a first approximation, their contribution can be separated based on theoretical considerations. The amount of sediments in a trap can be calculated as

$$m = \left(F_w t_{\text{tot}} + \sum_{i=1}^n F_i t_i \right) S, \quad (8)$$

Table 1. Horizontal sediment fluxes F_{tot} measured in summer 2009 near Katariina Jetty. The start date and time, sampling duration t_{tot} , depth of the sea z , number of passing ferries ($n_{\text{SS}} = \textit{SuperStar}$, $n_{\text{S}} = \textit{Star}$, $n_{\text{X}} = \textit{Viking XPRS}$) and the mean values of F_{tot} for the measuring series are shown. The values of the rightmost column are given in the following order: elevation from the sea bed $H = 0.5$ m seaward/shoreward; $H = 0.2$ m seaward/shoreward.

Date	Start time	t (h)	z (m)	n_{SS}	n_{S}	n_{X}	F_{tot} (g m ⁻² h ⁻¹)
18 June	16:34	2.5	2.3	1	0	0	1.2/1.3; 3.6/2.9
18 June	19:06	16.0	2.3	1	2	1	0.3/0.4; 1.9/2.0
19 June	11:22	6.6	2.3	1	1	1	0.8/1.3; 5.2/4.1
27 June	12:18	6.6	2.2	1	1	1	1.2/0.6; 7.1/6.7
27 June	18:52	16.6	2.2	1	1	1	0.2/0.6; 0.6/0.2
28 June	11:43	7.6	2.2	1	1	1	0.4/0.3; 5.5/5.8
20 July	21:48	9.5	4.2	0	1	1	0.4/0.1; 1.3/1.0
21 July	07:45	50.5	4.2	6	5	4	1.2/-; 1.4/2.5

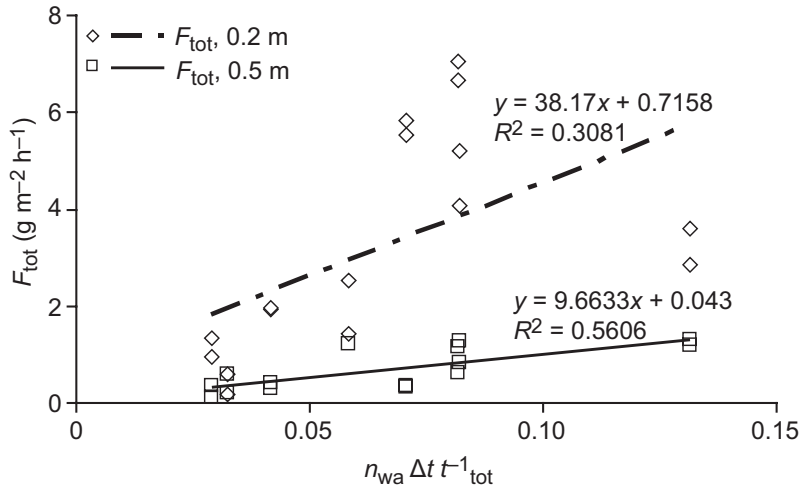


Fig. 8. Dependence of total horizontal sediment flux F_{tot} on the time proportion of ferries' impact $n_{\text{wa}} \Delta t / t_{\text{tot}}$ at 0.2 and 0.5 m from the sea bed.

where F_w is the wind waves' induced flux, F_i is the flux induced by a ship during the impact time t_i of its wake and n is the number of ships passing during t_{tot} . Combining Eqs. 7 and 8 we obtain:

$$\frac{m}{St_{\text{tot}}} = F_{\text{tot}} = F_w + \frac{1}{t_{\text{tot}}} \sum_{i=1}^n F_i t_i, \quad (9)$$

Wakes from three fast ferries arriving from Helsinki — *SuperStar* (SS), *Star* (S) and *XPRS* (X) — apparently give the major contribution to the flux. Other ships and the traffic in the Tallinn–Helsinki direction create much smaller waves at the measurement site (Fig. 3) and their contribution can be neglected. Consequently, the total flux can be approximated as follows:

$$F_{\text{tot}} = F_w + \frac{\Delta t}{t_{\text{tot}}} (n_{\text{SS}} F_{\text{SS}} + n_{\text{S}} F_{\text{S}} + n_{\text{X}} F_{\text{X}}), \quad (10)$$

where F_{SS} , F_{S} , F_{X} and n_{SS} , n_{S} , n_{X} are the mean fluxes (calculated for a period Δt equal for all the ferries) and number (during t_{tot}) of ferries passing. It is not possible to estimate the values of F_{SS} , F_{S} and F_{X} , from the existing data. From wave characteristics (Fig. 3c) one can estimate the wave induced orbital velocities for these ferries. As the intensity of resuspension is usually proportional to squared velocity, it is natural to assume that the concentration of resuspended particles at some height from the sea bed is proportional to square of orbital velocity. Therefore, Eq. 10 can be written as

$$F_{\text{tot}} = F_w + \frac{\Delta t}{t_{\text{tot}}} F_{\text{SS}} \left[n_{\text{SS}} + n_{\text{S}} \left(\frac{v_{\text{oS}}}{v_{\text{oSS}}} \right)^2 + n_{\text{X}} \left(\frac{v_{\text{oX}}}{v_{\text{oSS}}} \right)^2 \right], \quad (11)$$

$$= F_w + \frac{n_{\text{wa}} \Delta t}{t_{\text{tot}}} F_{\text{SS}}$$

where v_{oSS} , v_{oS} and v_{oX} are the near bottom orbital velocities induced by ferries (0.57, 0.36 and 0.27 m s⁻¹ respectively, *see* Fig. 3c) and n_{wa} is a weighted average of the number of ferries. A sensible approximation for Δt (about 22 min, Fig. 7b) could be taken from the analysis of the duration of response of the optical properties of sea water to the wakes. Based on the dataset of fluxes (Table 1), the dependence $F_{\text{tot}}(n_{\text{wa}} \Delta t / t_{\text{tot}})$ for the measuring elevations (0.2 and 0.5 m from the sea bottom) was calculated (Fig. 8), giving $F_w \approx 0.7$ (g m⁻² h⁻¹) and $F_{\text{SS}} \approx 38$ (g m⁻² h⁻¹) at the 0.2 m level, and $F_w \approx 0.05$ (g m⁻² h⁻¹) and $F_{\text{SS}} \approx 9.5$ (g m⁻² h⁻¹) at the 0.5 m level. The calculated values of F_w correlate well with the flux values at measurement series, when minimum proportion of ferries wakes is present (0.96–1.35 g m⁻² h⁻¹ at the 0.2 m level and 0.12–0.35 g m⁻² h⁻¹ at the 0.5 m level; *see* also Table 1).

Vertical fluxes of resuspended sediment showed a large variability (0.03–7.1 g m⁻² h⁻¹) depending on the deployment duration and the height of traps above the sea bed (Table 2). Significant downwelling fluxes were registered at the 0.5 m level above the sea bed and not at higher elevations. There was also a quite good

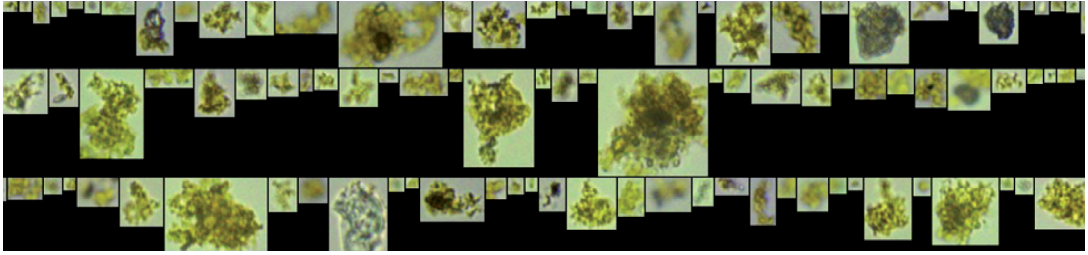


Fig. 9. Examples of microphotos of counted particles.

correlation between the mean values of vertical and horizontal fluxes for the same measuring cycle.

Although the presented estimates are very rough, they show that in calm and moderate wind wave conditions (for example, during a large part of the spring and summer seasons) the role of wind waves is marginal in the resuspension process ($\sim 2\%$ at the 0.2 m level and $\sim 0.05\%$ at the 0.5 m level). Also, the measurements clearly showed that the fluxes are strongly depending on the elevation.

Size and distribution of particles in resuspended sediments

The FlowCAM analysis was carried out for two reasons. First, there are many investigations addressing the dependence of attenuation on the concentration of optically active substances (OAS) in natural waters but the question concerning the size and morphology of particles is still open. Second, the samples had very clear

orange shading, which was not characteristic on other shores of Tallinn Bay.

As fluorescence measurements were not carried out, all particles (tripton, phytoplankton, zooplankton, and detritus) were considered in the FlowCAM analysis. Invalid recordings (i.e. bubbles and repeated images) were removed from the image database through visual recognition. About 2700–3800 particles were counted in the 5 ml samples. Most of them had an irregular shape but the same colour and structure — yellow-green background with very fine black spots inside (Fig. 9). The orange colour of (macro) samples may be due to a fine iron-rich sand fraction or to red brick pebbles originated from the facilities established on Cape Väike-Paljassaar during World War I.

Particle diameter distributions (ESD) in real downwelling fluxes ($\text{m}^{-2} \text{h}^{-1}$) were studied using a $5 \mu\text{m}$ step. These distributions were quite similar for all the samples (Fig. 10). Although the studied particles varied from 2 to $150 \mu\text{m}$ in diameter, in 90% cases the diameters were in the range of $2\text{--}40 \mu\text{m}$.

Table 2. Vertical sediment fluxes F_{vert} measured in summer 2009 near Katariina Jetty. The date, end and start times, sampling duration t_{tot} , depth of the sea z , elevation from the sea bed H and the mean values of F_{vert} for the measuring series are shown. The values of the rightmost column are given in the following order: elevation from the sea bed 1.1/0.9/0.8/0.5 m.

Date	Start time	t_{tot} (h)	z (m)	F_{vert} ($\text{g m}^{-2} \text{h}^{-1}$)
18 June	16:37	2.6	3.1	0.2/0.4/0.4/1.5
19 June	11:22	6.6	3.1	0.1/0.2 /0.2/3.2
27 June	19:20	16.0	2.4	0.1/0.9 /3.2/7.1
16 July	14:33	2.6	3.25	0.1/0.2 /0.4/0.4
21 July	08:26	49.8	3.6	0.03/0.03/0.04/0.06

Conclusions

Wakes from fast ferries dominated the surface wave field during the experiment. The daily highest wake waves were at least 0.65 m high and their period was 7–8 s. They induced near-bottom orbital speeds of 0.5 m s^{-1} and more. Compared with measurements made at eastern coast of Tallinn Bay, the wakes were slightly lower, but their period was the same. This suggests that although the ship wave height may vary in different locations, the periods of the largest waves in wakes of *Tallink Star*, *Tallink*

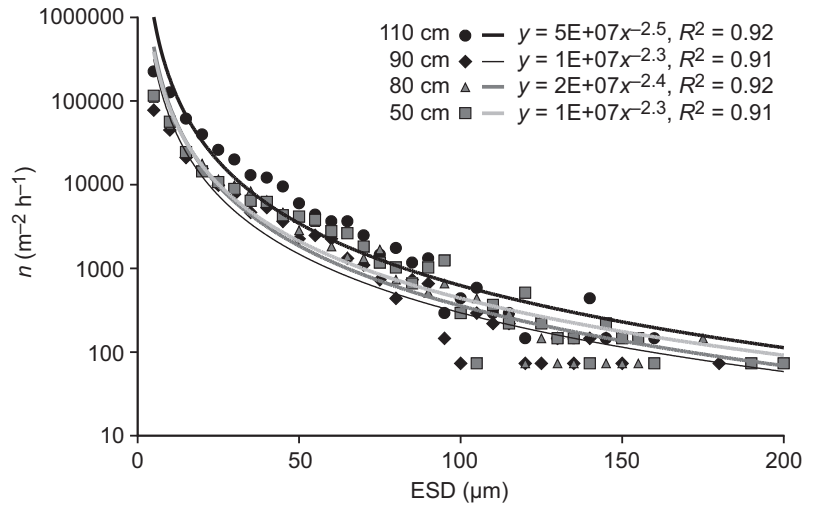


Fig. 10. Distribution of diameters of sediment particles sampled from several horizons from the sea bed in 50.5 h period on 21–23 July 2009 (ESD = equivalent spherical diameter).

SuperStar and *Viking XPRS* insignificantly varies in the entire bay. This is consistent with the general opinion that the wave period depends mainly on the ship's speed, characteristics and water depth at the generation area. Model experiments with the numerical model SWAN indicated, that the daily maximum wake induced flow velocities are comparable with the velocities generated by north winds with a speed of 12 m s^{-1} or SW winds with a speed of 18 m s^{-1} .

Optical cross section for the suspended matter at 502 nm $K'_{d,s,502}$ was found to be $0.1 \text{ m}^2 \text{ g}^{-1}$ in Tallinn Bay. The response of optical parameters of sea water to the wake from *SuperStar* was about 1.7 times as high as was observed for HSC during the measurements made at Aegna Island in 2003 and 2004. The similar response to wakes from other ferries, calculated using the orbital velocities of their waves, had lower impact. The typical impact of the wake from *Star* forms about 40% and of the wake from *XPRS* about 20% of the impact of *SuperStar*'s wake. The mean excess concentrations of resuspended sediments induced by a ferry wake were 2.0 , 0.8 and 0.4 g m^{-3} for *SuperStar*, *Star* and *XPRS*, respectively. Therefore, only the impact of the wake from *SuperStar* is of the same magnitude as the similar impact exerted by wakes of 'classic' high-speed crafts such as *Autoexpress* and *SuperSeaCat* (Soomere *et al.* 2003, Parnell *et al.* 2008), the wakes from which dominated in the ship-induced hydrodynamic activity in the past. The daily 'total impact' of all ferries was $10\,350 \text{ g s m}^{-3}$, that is about one

third of the analogous value for the nearshore of Aegna in 2003–2004. The amount of sediments which may be carried out of the bay or accumulated in deeper sea areas during one navigation period is about 400 kg per meter of shoreline, which is about 2.5 times lower than estimated for year 2005 near Aegna.

The data obtained from horizontal sediment traps showed slight sediment transport away from the shore. The absolute majority of resuspension events were caused by ship wakes. They induced resuspension higher as induced by wind waves about 50 times at the 0.2 m level and about 200 times at the 0.5 m level from the sea bed. The magnitude of sediment fluxes very strongly depends on the elevation from the sea bed. The horizontal fluxes induced by ferry wakes at the 0.5 m level were 4 times as large as at the 0.2 m level. This difference for fluxes induced by wind waves was 14-fold. Vertical fluxes of resuspended sediments showed a large variability (0.03 – $7.1 \text{ g m}^{-2} \text{ h}^{-1}$), depending on the time period and elevation of the traps from the sea bed. Significant downwelling fluxes were registered at the 0.5 m level from the sea bed but not at higher elevations. This means that the maximum effective resuspension height of particles due to ferry wakes is between 0.5 – 0.8 m .

The diameters of resuspended sediment particles ranged from 2 – $150 \mu\text{m}$, remaining in 90% of cases in the range of 2 – $40 \mu\text{m}$.

The quantitative estimates discussed above suggest that remarkable amounts of sediment

may be lost from the shoreline due to fast ferries every year. The process apparently will continue in the future and therefore may seriously affect sediment dynamics.

Acknowledgments: This study was financially supported by Estonian Science Foundation grants no. 7000, 7283 and by contract EMP 53. We are very grateful to four anonymous referees for their critical comments and suggestions.

References

- Alari V. & Raudsepp U. 2010. Depth induced breaking of wind generated surface gravity waves in Estonian coastal waters. *Boreal Env. Res.* 15: 295–300.
- Alari V., Erm A. & Raudsepp U. 2009a. Anthropogenic storms in the Baltic Sea and the coastal response. In: *11th Workshop on wave hindcasting and forecasting & 2nd Coastal hazards symposium, October 18–23, 2009, Halifax, Canada, JCOMM Techn. Rep. Ser. 52*, available on the web at <http://www.waveworkshop.org/11thWaves/Papers/Anthropogenic%20storms%20in%20the%20Baltic%20Sea%20and%20the%20coastal%20response.pdf>.
- Alari V., Raudsepp U., Kõuts T., Erm A. & Vahter K. 2009b. On the validation of SWAN, a third generation spectral wave model, in Estonian coastal waters. In: *BSSC 2009, August 17–21, 2009, Tallinn, Estonia, Abstract Book*, Tallinn University of Technology, p. 183.
- Binding C.E., Bowers D.G. & Mitchelson-Jacob E.G. 2003. An algorithm for the retrieval of suspended sediment concentrations in the Irish Sea from SeaWiFS ocean colour satellite imagery. *Int. J. Remote Sens.* 24: 3791–3806.
- Binding C.E., Bowers D.G. & Mitchelson-Jacob E.G. 2005. Estimating suspended sediment concentrations from ocean colour measurements in moderately turbid waters; the impact of variable particle scattering properties. *Rem. Sens. Env.* 94: 373–383.
- Booij N., Ris R.C. & Holthuijsen L.H. 1999. A third generation wave model for coastal regions. 1. Model description and validation. *J. Geophys. Res.* C104: 7649–7666.
- Booth J.G., Miller R.L., McKee B.A. & Leathers R.A. 2000. Wind-induced bottom sediment resuspension in a microtidal coastal environment. *Cont. Shelf Res.* 20: 785–806.
- Dera J. 1992. *Marine physics*. PWN, Warszawa and Elsevier, Amsterdam.
- Devlin M.J., Barry J., Mills D.K., Gowen R.J., Foden J., Sivyer D., Greenwood N., Pearce D. & Tett P. 2009. Estimating the diffuse attenuation coefficient from optically active constituents in UK marine waters. *Estuar. Coast. Shelf Sci.* 82: 73–83.
- Didenkulova I.I., Pelinovsky E.N. & Soomere T. 2009. Can the waves generated by fast ferries be a physical model of tsunami? In: *24th International Tsunami Symposium, July 14–16, 2009, Technical Workshop on Tsunami Measurements and Real-Time Detection, July 17, 2009, Novosibirsk, Russia, Programme and Abstracts*, ICMG SB RAS, Novosibirsk, p. 68.
- Dierssen H.M., Zimmerman R.C. & Burdige D.C. 2009. Optics and remote sensing of Bahamian carbonate sediment whittings and potential relationship to wind-driven Langmuir circulation. *Biogeosciences* 6: 487–500.
- Effler S.W., Perkins M., Ohrazda N., Matthews D.A., Gelda R., Peng F., Johnson D.L. & Stepchuk C.L. 2002. Tripton, transparency and light penetration in seven New York reservoirs. *Hydrobiologia* 468: 213–232.
- Erm A. & Soomere T. 2004. Influence of fast ship waves on the optical properties of sea water in Tallinn Bay. *Proc. Estonian Acad. Sci. Biol. Ecol.* 53: 161–178.
- Erm A. & Soomere T. 2006a. The impact of fast ferry traffic on underwater optics and sediment resuspension. *Oceanologia* 48(S): 283–301.
- Erm A. & Soomere T. 2006b. Optical detection of sediment resuspension by wakes from fast ferries. In: Lukševičs E., Kalnina L. & Stinkulis G. (eds.), *The Baltic Sea Geology: The 9th Marine Geological Conference, Jurmala, Latvia, 2006*, University of Latvia, Riga, pp. 25–28.
- Erm A., Kask A. & Soomere T. 2006. Optical model for monitoring resuspension of the bottom sediments. In: Tubielewicz A. (ed.), *Coastal Environment, Processes and Evolution: Eurocoast – Littoral 2006*, Gdansk, Gdansk University of Technology, pp. 150–157.
- Erm A., Alari V. & Kõuts T. 2008. Transport of sediments resuspended by ferries. In: *US/EU-Baltic International Symposium, 2008 IEEE/OES: US/EU-Baltic International Symposium, Tallinn, Estonia, 27–29 May 2008*, IEEE Conference Proceedings, doi:10.1109/BALTIC.2008.4625546.
- Erm A., Alari V. & Listak M. 2009. Monitoring wave-induced sediment resuspension. *Estonian J. Eng.* 15: 196–211.
- Floderus S., Jahmlich S., Ekeboom J. & Saarlo M. 1999. Particle flux and properties affecting the fate of bacterial productivity in the benthic boundary layer at a mud-bottom site in South-Central Gulf of Riga. *J. Mar. Syst.* 23: 233–250.
- Jõevere K. 2003. Kiirlaevade lained ohustavad randades väikesi suplejaid. *Eesti Päevaleht* 178 (5 Aug. 2003).
- Jönsson A. 2006. A model study of suspended sand due to surface waves during a storm in the Baltic Proper. *J. Mar. Syst.* 63: 91–104.
- Kelpšaitė L. & Soomere T. 2009. Vessel-wave induced potential longshore sediment transport at Aegna Island, Tallinn Bay. *Estonian J. Eng.* 15: 168–181.
- Kink H. & Raukas A. (ed.) 1998. *Natural heritage of Estonia. 3. Northern Tallinn, Haabersti*. Tallinn Naturalists' Society, Tallinn Environment Department, Institute of Geology at TUT, Estonian Academy Publishers.
- Kurennoy D., Soomere T. & Parnell K.E. 2009a. Variability in the properties of wakes generated by high-speed ferries. *J. Coast. Res. Special Issue* 56: 519–523.
- Kurennoy D., Didenkulova I. & Soomere T. 2009b. Crest-trough asymmetry of waves generated by high-speed vessels. *Estonian J. Eng.* 15: 182–195.
- Lawrence F.S. & Herbert C.Jr. 1968. The relative contribution of particulate chlorophyll and river tripton to the

- extinction of light off the coast of Oregon. *Limnol. Oceanogr.* 13: 84–91.
- Orlenko L.R. [Орленко Л.Р.] (ed.) 1984. [*Studies of the hydrometeorological regime of Tallinn Bay*]. Gidrometeoizdat, Leningrad. [In Russian].
- Parnell K.E., Delpêche N., Didenkulova I., Dolphin T., Erm A., Kask A., Kelpšaitė L., Kurennoy D., Quak E., Räämet A., Soomere T., Terentjeva A., Torsvik T. & Zaitseva-Pärnaste I. 2008. Far-field vessel wakes in Tallinn Bay. *Estonian J. Eng.* 14: 273–302.
- Peltoniemi H., Bengston A., Rytkönen J. & Kõuts T. 2002. Measurements of fast ferry waves in Helsinki–Tallinn route. In: *The changing state of the Gulf of Finland ecosystem, Tallinn, 2002, Abstracts*, Estonian Ministry of Environment, Tallinn, p. 23.
- Prilipko G.I. [Прилипко Г.И.] (ed.) 1982. [*Climate of Tallinn*]. Gidrometeoizdat, Leningrad. [In Russian].
- Saarse L. & Vassiljev J. 2008. Kopli ja Paljassaare poolsaar olid veel hiljaegu saared. *Eesti Loodus* 59: 536–539.
- Sieracki C.K., Sieracki M.E. & Yentsch C.S. 1998. An imaging-in-flow system for automated analysis of marine microplankton. *Mar. Ecol. Prog. Ser.* 168: 285–296.
- Smith R.C. & Baker K.S. 1981. Optical properties of the clearest natural waters (200–800 nm). *Appl. Optics* 20/2: 177–184.
- Soomere T. 2005a. Wind wave statistics in Tallinn Bay. *Boreal Env. Res.* 10: 103–118.
- Soomere T. 2005b. Fast ferry traffic as a qualitatively new forcing factor of environmental processes in non-tidal sea areas: a case study in Tallinn Bay, Baltic Sea. *Environ. Fluid Mech.* 5: 293–323.
- Soomere T. 2006. Nonlinear ship wake waves as a model of rogue waves and a source of danger to the coastal environment: a review. *Oceanologia* 48(S): 185–202.
- Soomere T. & Kask J. 2003. A specific impact of waves of fast ferries on sediment transport processes of Tallinn Bay. *Proc. Estonian Acad. Sci. Biol. Ecol.* 52: 319–331.
- Soomere T. & Rannat K. 2003. An experimental study of wind and ship waves in the Tallinn Bay. *Proc. Estonian Acad. Sci. Eng.* 9: 157–184.
- Soomere T., Rannat K., Elken J. & Myrberg K. 2003. Natural and anthropogenic wave forcing in the Tallinn Bay, Baltic Sea. In: Brebbia C.A., Almorza D. & Lopez-Aguayo F. (eds.), *Coastal Engineering VI: Computer Modelling and Experimental Measurements of Seas and Coastal Regions*, Wessex Institute of Technology Press, Southampton, Boston, pp. 273–282.
- Soomere T., Pöder R., Rannat K. & Kask A. 2005. Profiles of waves from high-speed ferries in the coastal area. *Proc. Estonian Acad. Sci. Eng.* 11: 245–260.
- Sterling M.C.Jr., Bonner J., Ernest A.N.S., Page C.A. & Autenrieth R.L. 2004. Characterizing aquatic sediment-oil aggregates using in situ instruments. *Mar. Pollut. Bull.* 48: 533–542.
- Torsvik T. & Soomere T. 2008. Simulation of patterns of wakes from high-speed ferries in Tallinn Bay. *Estonian J. Eng.* 14: 232–254.
- Torsvik T., Didenkulova I., Soomere T. & Parnell K.E. 2009. Variability in spatial patterns of long nonlinear waves from fast ferries in Tallinn Bay. *Nonlinear Processes in Geophysics* 16: 351–363.
- Van der Westhuysen A.J., Zijlema M. & Battjes J.A. 2007. Nonlinear saturation-based whitecapping dissipation in SWAN for deep and shallow water. *Coast. Eng.* 54: 151–170.
- Wild-Allen K., Lane A. & Tett P. 2002. Phytoplankton, sediment and optical observations in Netherlands coastal waters in spring. *J. Sea Res.* 47: 303–315.